Proc. Natl. Acad. Sci. USA
Vol. 93, pp. 7013–7016, July 1996
Biophysics

X-ray structure determination of a metastable state of carbonmonoxy myoglobin after photodissociation

(protein dynamics/r/t-transition/low temperature structure)

H. HARTMANN†, S. ZINSER†, P. KOMNINOS‡, R. T. SCHNEIDER§, G. U. NIENHAUS¶, AND F. PARAK‡‖

†Institute für Molekulare Biophysik, Johannes-Gutenberg Universität, Jakob Welder Weg 26, D-55099 Mainz, Germany; ‡Fakultät für Physik, E17, Technische Universität München, D-85747 Garching, Germany; §European Molecular Biology Laboratory Outstation Hamburg, c/o Deutsches Elektronen Synchrotron, Notkestrasse 85, Geb. 25A, D-22603 Hamburg, Germany; and ¶Department of Physics, University of Illinois at Urbana–Champaign, 1110 West Green Street, Urbana, IL 61801

Communicated by Hans Frauenfelder, Los Alamos National Laboratory, Los Alamos, NM, March 14, 1996 (received for review July 7, 1994)

ABSTRACT **The x-ray structure of carbon monoxide (CO)-ligated myoglobin illuminated during data collection by a laser diode at the wavelength λ = 690 nm has been determined to a resolution of 1.7 A at T = 36 K. For comparison, we also measured data sets of deoxymyoglobin and CO-ligated myoglobin. In the photon-induced structure the electron density associated with the CO ligand can be described by a tube extending from the iron into the heme pocket over more than 4 A. This density can be interpreted by two discrete positions of the CO molecule. One is close to the heme iron and can be identified to be bound CO. In the second, the CO is dissociated from the heme iron and lies on top of pyrrole ring C. At our experimental conditions the overall structure of myoglobin in the metastable state is close to the structure of a CO-ligated molecule. However, the iron has essentially relaxed into the position of deoxymyoglobin. We compare our results with those of Schlichting *et al.* [Schlichting, I., Berendzen, J., Phillips, G. N., Jr., & Sweet, R. M. (1994) *Nature* 317, 808–812], who worked with the myoglobin mutant (D122N) that crystallizes in the space group P6 and Teng *et al.* [Teng, T. Y., Srajer, V. & Moffat, K. (1994) *Nat. Struct. Biol.* 1, 701–705], who used native myoglobin crystals of the space group $P2_1$. Possible reasons for the structural differences are discussed.**

Enzymes and proteins that transport small molecules normally exist in two conformations: the ligated conformation and the unligated conformation. In general, x-ray structure analysis is able to distinguish the structural differences. However, for many years it has been impossible to obtain direct structural information on intermediate states occupied during conformational transitions. The existence of such states is well known from spectroscopic techniques. Several groups have concentrated their investigations on myoglobin. Fundamental experiments have been performed on carbon monoxide (CO)-ligated myoglobin (MbCO) (1–3). After flash photolysis the CO cannot escape from the heme pocket at temperatures below 180 K. The rebinding kinetics of the CO reveals intermediate states, denoted Mb*CO. The power law kinetics show that the Mb*CO molecules have slightly different barriers for the rebinding of the CO to the heme iron and represent, therfore, a multiplicity of conformations, often called conformational substates. This picture is supported by IR spectroscopy (4) and Mössbauer spectroscopy (5).

The first attempts to obtain direct structural information on these intermediate states have been performed by the technique of dispersive x-ray absorption (6–10). Recently, two groups have reported x-ray structure determination of Mb*CO at 20 K (11) and 40 K (12). At these low temperatures, recombination after photodissociation is very slow, so that continuous illumination of the crystal with visible light during x-ray exposure leads to an efficient conversion of MbCO to the photoproduct Mb*CO. Schlichting and collaborators (11) used crystals of a myoglobin mutant (D122N) at pH 9 in the P6 space group, whereas Teng *et al.* (12) employed standard monoclinic crystals of native MbCO at pH 6.0. The two structures are surprisingly different in the relevant structural details. Here we present a third, independent x-ray structure analysis where MbCO and Mb*CO are present in the same sample, compare the results, and discuss possible reasons for the discrepancies between the structures.

Materials and Methods

Sperm whale metmyoglobin (Mbmet) crystals were grown in the space group $P2_1$ at pH 6.2 according to the method of Kendrew and Parrish (13). To obtain the deoxymyoglobin form (Mb) the crystals were soaked in an ammonium sulfate solution. Small crystals ($0.3 \times 0.4 \times 0.5$ mm^3) were mounted in glass capillaries and sealed. The preparation of the MbCO crystals was done in the same way, but in CO gas with CO saturated ammonium sulfate solution. Mb or MbCO crystals were dissolved in degassed buffer at pH 6.2 and optical spectra were measured. No indiction of Mbmet was found. For the low temperature experiments the crystals were shock frozen in liquid propane (14) and loaded into a cryostat modified for liquid helium operation (15). The cryostat was mounted on a two-axis goniometer. The Mb*CO data set was recorded with a Marresearch imaging plate detector at the beamline X11 of the European Molecular Biology Laboratory outstation at Deutsches Elektronen Synchrotron using an x-ray wavelength of 0.9 A. During the whole data collection the crystal was illuminated with a red laser diode (Toshiba, 20 mW, 690 nm) focused to a spot of 1 mm in diameter at the position of the crystal to photodissociate the CO from the heme iron. According to Bücher and Kaspers (16) the quantum efficiency for dissociation should be close to one even at λ = 690 nm. The calculated photolysis rate should then be between 1 and 10 s^{-1}. Passing the crystal the light intensity is reduced to about 0.5 of the incoming intensity. A complete photolysis is expected under those conditions. Measurements were started after about 5 min of illumination. After about 2 hr of data collection with continuous illumination corresponding to a rotation of about 20 degrees, the laser was switched off for about 2 min to check if the crystal was still correctly aligned with respect to the x-ray beam. Then the measurement started again for 2 hr. The data were reduced with DENZO (17). All other data sets were collected with a multiwire proportional counter (18) using MoK_α radiation from either a conventional x-ray source or a rotating anode generator and reduced with the program FILME (19). The refinement was done using the program PROLSQ (20). The Mbmet structure at 300 K

The publication costs of this article were defrayed in part by page charge payment. This article must therefore be hereby marked "*advertisement*" in accordance with 18 U.S.C. §1734 solely to indicate this fact.

Abbreviations: Mb, deoxymyoglobin; MbCO, CO-ligated myoglobin; Mbmet, metmyoglobin.

‖To whom reprint requests should be addressed.

(21) was used as a starting model in the refinement of the MbCO and the Mb structures at 300 K. The MbCO at 300 K was then used as the initial coordinate set for the refinement of MbCO at 90 K, which in turn served as input for the refinement of the Mb*CO structure at 36 K. In the model for Mb at 300 K we included two x-ray visible sulfate anions. For the refinement of the CO structures, additional water positions generated by a Monte Carlo method were used (22). These waters have a B-value of about 50 A^2 and are, therefore, crystallographically invisible. It was shown that this more realistic model for the solvent region also improves the quality of maps in the protein part. Because in refs. 11 and 12 no Monte Carlo waters were used, we also refined our data without these waters. This way we proved that the conclusions drawn in the following discussion do not depend on the different refinements. The total number of solvent molecules, including the two located sulfate groups, was about 400 per Mb molecule. Coordinates and individual B-values were refined for all atoms, occupancies only for the solvent atoms and for the two positions of the CO in the Mb*CO structure. Occupancies and B-values are, of course, strongly correlated. Nevertheless, this treatment gives an optimal average electron density between the protein molecules. It would not be suitable for a discussion of the coordinates of water molecules. The positions of the CO in MbCO and the distal water molecule in Mbmet were initially not restrained to the iron or any other part of the protein, neither by bonded nor by nonbonded interactions. This means that, in contrast to the common practice, they were allowed to move freely in the electron density. Because we obtained remarkable deviations from published values for the position of the bound CO in MbCO (23), we repeated the calculations with the distance Fe—C of 1.8 A and a restraint σ = 0.02 A. With the restraints, we obtained practically the same Fe—CO distance as in ref. 23. However, we found no indications for different CO binding angles at our resolution. At several stages of the refinement difference and omit maps were calculated to localize solvent molecules and to correct manually misplaced side chains, especially in the refinement of the deoxy structure. Table 1 summarized some technical details of the structure determinations.

Structural Changes in the Photoproduct

The most pronounced change that we observe upon illumination of the MbCO crystal is associated with the electron density of the CO ligand. In Mb*CO at 36 K this feature can be described by a tube that extends from the heme iron more than 4 A into the heme pocket (Fig. 1). This density distribution is incompatible with a single position of the CO, but can be fitted perfectly with two discrete CO positions. Unconstrained refinement resulted in occupancies of 0.45 for position 1 near the heme iron, and 0.62 for the position 2 on top of pyrrole ring C. The two numbers do not add up to 1 because no restraints were applied between the two positions. Normalization yields 42% occupation for position 1 and 58% occupation for position 2. Difference maps show no other features in the heme pocket above the noise level. Therefore, other significantly populated positions of the CO in the heme pocket at 36 K are unlikely. Our electron density map does not allow us to distinguish whether the carbon or the oxygen atom of the CO is closer to the heme iron. Isotope effects of the rebinding of CO by molecular tunneling at low temperatures suggest that the C atom is closer to the iron (25). For our structure and the data compiled in Table 2 we assume the C atom to be always closer to the heme iron.

For position 1 in Mb*CO, we obtain an Fe—C distance of 2.27 A. From a comparison with small model compounds (e.g.,

Table 1. Parameters of the evaluation and the refinement

	MbCO (300 K)	MbCO (90 K)	Mb*CO (36 K)	Mb (300 K)
Data evaluation				
N_{obs}	13,000	11,398	11,908	11,341
Resol. [A]	1.7	1.7	1.7	1.7
Compl. (%)	87.5	76.8	80.1	76.3
R_{merge}	8.1	10.5	6.9	7.4
Refinement				
N_{ref}	12,370	10,646	11,264	11,329
R_{cryst}	17.7	15.1	15.5	15.5
Res_{ref} [A]	14.8-1.7	15.6-1.7	8.4-1.7	10.2-1.7
rms err [A]	0.19	0.17	0.16	0.17
Structural geometry				
Bond lengths				
dist. σ [A]	0.020	0.015	0.015	0.020
dist. Δ [A]	0.021	0.016	0.018	0.018
Bond angles				
angl. σ_w [A]	0.040	0.060	0.060	0.040
angl. Δ [A]	0.054	0.083	0.072	0.048

N_{obs}, number of observed unique reflections; Resol., measured resolution; Compl., completeness of measurement; $R_{merge} = \Sigma \mid I - \langle I \rangle \mid \Sigma \langle I \rangle$. N_{ref}, number of reflections used for the refinement; $R_{cryst} = \Sigma \mid F_0 - F_c \mid / \Sigma F_0$; Res_{ref}, resolution range used for the strength of the restraint; rms err., upper limit for rms coordinate error estimated from Luzzati plots (24). Δ, rms deviation from the standard values.

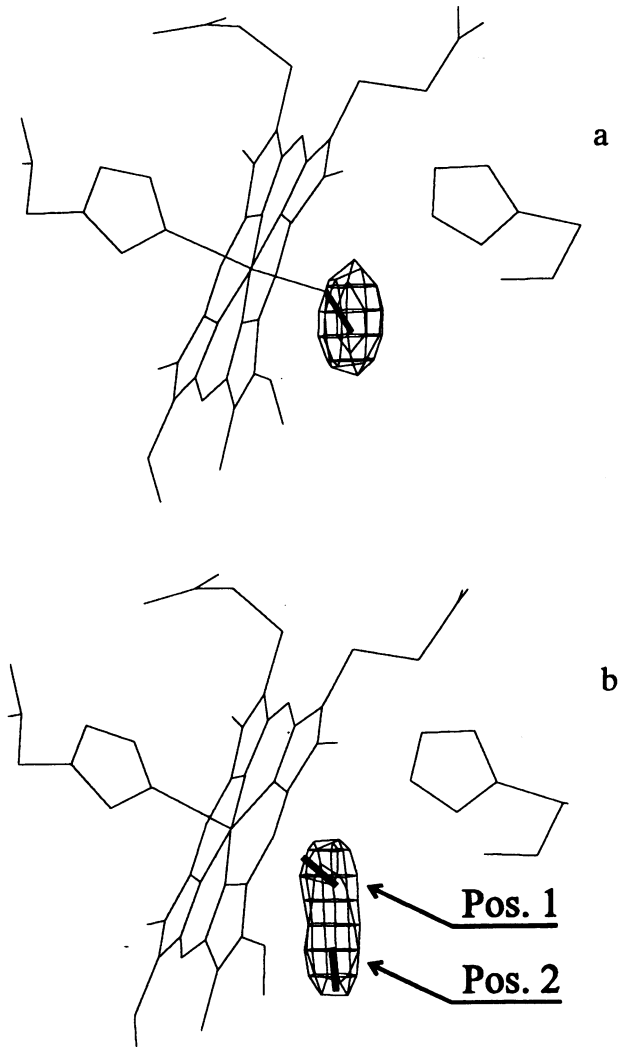

FIG. 1. Electron density obtained by a Fourier transformation of F^0 (MbCO) − F^c (MbCO-CO). F^0 are the structure factors of the MbCO structure with observed intensities and calculated phases. F^c is calculated from the MbCO structure omitting the CO molecule. The density is contoured at a level of 6σ. Coordinates from the restrained refinements are used: (*a*) MbCO at 90 K. (*b*) Mb*CO at 36 K. The heme group and the distal and proximal histidine are drawn for orientation.

Table 2. Comparison of x-ray structures of MbCO, Mb*CO, and Mb determined by different groups

	This work				Ref. 11			Ref. 12	Ref. 28*	Ref. 27*
	MbCO T = 300 K		Mb*CO T = 36 K	Mb T = 300 K	MbCO T = 85 K	Mb*CO T = 20 K	Mb T = 85 K	Mb*CO T = 40 K	MbCO T = 260 K	MbCO T = 295 K
Fe-PPIX	0.08		0.23	0.37	0.05	0.27	0.32		0.04	0.12
[A]	(0.07)		(0.22)	0.40*†						
Fe-CO	2.24	Pos 1:	2.27	—	1.85			2.60‡	1.92	2.12
[A]	(1.90)		(1.87)							
		Pos 2:	3.71	—		3.60				
Fe..OC	3.03	Pos 1:	3.08	—	2.93				2.93/2.73	3.19/3.08
[A]			(2.80)	—						
		Pos 2:	4.72			4.14				
β	120	Pos 1:	123	—	160			129	141/120	146/135
[°]	(141)		(139)							
"bend"		Pos 2:	144			111				
Θ	13	Pos 1:	12	—	4				3	14
[°]	(10)		(4)							
"tilt"		Pos 2:	30			39				

Fe-PPIX: Fe out of plane distance, the hemeplane PPIX is defined as the least-squares plane through the 20 central C atoms of the heme; FeCO, Fe. . .OC: distances of the C and the O atom of CO to the iron, respectively; bend angle β: the angle of Fe—C—O; tilt angle Θ: between Fe—C and the heme normal. In this paper the Fe—CO distance was calculated without restraint and with a restrained Fe—C distance of 1.8 A and $\sigma = 0.02$ *A*. The results obtained with this restraint are given in brackets.

*Values calculated from the corresponding Brookhaven PDP entries. Fe-PPIX and Θ depend somewhat on the definition of the mean hemplane (with or without the four nitrogen atoms).

†Value taken from ref. 26.

‡Estimated from the Fe—CO distance at 300 K and the shift of the CO given in ref. 12.

Fe—C = 1.77 A in ref. 27) one may come to the conclusion that the CO is unbound in position 1 but close to the heme iron. However, in our MbCO structure at T = 300 K refined without a restraint on the ligand position, we obtain a Fe—C distance of 2.24 A, which is nearly the same as in Mb*CO. If we restrain the CO, the Fe—C distance is 1.87 A in the photoproduct structure and 1.90 A in MbCO. Because the bound CO and the CO in position 1 behave so similarly, it is likely that we are dealing with a fraction of bound ligand in the photoproduct structure. Visual inspection shows that the models obtained with unrestrained refinements fit the observed electron densities clearly better. Rather large Fe—C distances have been reported previously in a neutron structure of MbCO (Fe—C = 2.12 A) (28) and in an x-ray structure of CO ligated chironomus hemoglobin (Fe—C = 2.4 A) (26). Kuriyan *et al.* (23) also mentioned that the Fe—C distance increased from 1.92 to 2.27 A in a few cycles of unrestrained refinement. In position 2, the Fe—C distance is 3.71 A, and therefore, the covalent protein–ligand bond is clearly broken. It should be mentioned that in Mb a water molecule occupies a position just between the flashed off and the bound CO in Mb*CO.

Another pronounced difference between the photoproduct and the bound-state structure is the iron displacement from the mean heme plane by 0.23 A. If we assume a superposition of 42% MbCO and 58% Mb*CO, we can use the value of 0.08 A for the iron displacement in MbCO to calculate the heme iron out-of-place distance of the pure Mb*CO species as 0.34 A. This shows that the iron is substantially displaced from the mean heme plane in Mb*CO, but has probably not reached the Mb position, which is at least 0.37 A out of plane. However, the limited accuracy of the data does not allow an unambiguous conclusion.

Except for the heme region, the overall structure of Mb*CO is very close to that of MbCO. Since Schlichting *et al.* (11) reported a displacement of the distal histidine (H64) imidazole side chain away from the ligand binding site upon photolysis, we carefully inspected the position of the distal histidine in our structure. We were not able to detect any changes in the position of the imidazole ring, either from the refined coordinates or from difference or omit maps.

Comparison with Previous Structure Determinations

The previous structure determinations by Schlichting *et al.* (11) and Teng *et al.* (12) clearly disagree with each other in the structural changes that were obtained upon photolysis. Schlichting *et al.* worked under continuous illumination at 20 K and found a single CO position with a Fe—C distance of 3.6 A that agrees with our position 2. They also reported a substantial displacement of the heme iron by 0.27 A, which amounts to 80% of the deoxy value. By contrast, Teng *et al.* report an increase of the Fe—C distance by only 0.7 A at 40 K. If we use our Fe—C distance of 1.90 A of MbCO, which agrees well with the value 1.85 A reported by Schlichting *et al.* (11), to calculate a Fe—C distance, we arrive at 2.60 A, which is just 0.33 A more than the Fe—C distance 2.27 A of our position 1.

Could it be possible that there are indeed different locations of the photodissociated CO that depend on photolysis protocol, temperature, or even crystal packing differences? Infrared spectroscopy gives strong indication against this possibility. In glycerol water solutions at pH 9, one stretch band of the photodissociated CO at 2131 cm^{-1} in the heme pocket dominates above 20 K (29). The same is true for crystalline preparations of both D122N mutant MbCO in hexagonal crystals and native MbCO in monoclinic crystals (G.U.N., unpublished results), suggesting that the heme pocket at low temperature is very similar in crystals and solutions. In recent years it has become clear that CO is a sensitive gauge of electrostatic fields in the heme pocket (30), which should be markedly different for the different positions. Indeed, below 20 K transitions of the CO between 2118 and 2131 cm^{-1} have been observed and interpreted as movements of the CO in the heme pocket (29). However, near 40 K the infrared data do support the presence of only one dominant location of the photodissociated CO in the heme pocket.

How can we then understand the observed multiple positions of the CO resulting from the x-ray data? An obvious explanation is that the positions close to the heme iron are due to bound and not photodissociated CO in the heme pocket. This scenario would imply either insufficient illumination, so that part of the crystal was never photolyzed, or that recombination was too fast to keep the CO off the heme iron. Our estimations given before indicate that there should be complete dissociation. However, they are by no means very accurate. One should also be aware that the photolysis light source can significantly heat up the crystal. The temperature of the crystal under illumination is certainly higher than the quoted

temperatures of the environment. Rebinding is a thermally activated process, and sample heating will lead to a significant increase of the rebinding rates. Schlichting *et al.* (11) worked at the lowest temperature of the three structure determinations, namely ≈20 K, so that the smallest problems with incomplete photolysis should be expected. Indeed, these authors find no evidence for a position of the CO near the heme iron.

An additional problem arises from the fact that MbCO has three different A substates (31), which have different enthalpy barrier distributions and, therefore, rebind with different kinetics (32). The relative populations of the A_0 and A_1 substates depend on pH, with A_1 dominating at high pH. In P6 and $P2_1$ crystals, A_0 is characterized by an enthalpy barrier distribution peaking at about 6 kJ/mol, whereas A_1 peaks around 10 kJ/mol (G.U.N., unpublished results). Consequently, A_0 rebinds much faster. Schlichting *et al.* (11) used crystals at pH 9, which minimizes the A_0 substate population. Teng *et al.* (12) used crystals grown at pH 6.0, whereas ours were grown at pH 6.2. They contain already between 10 and 20% of the faster A_0 state. If the preparation is not performed completely anaerobically, the reaction of dithionite with oxygen does not only lead to incomplete reduction, but also lowers the pH and yields an even larger fraction of A_0. The similar structural properties of the CO in MbCO and position 1 in Mb*CO in our data suggests the presence of bound CO in our structure. We consider it likely that the data presented by Teng *et al.* (12) can also be explained by assuming only a small fraction of photoproduct, leading to a smaller iron displacement and the inability to refine the position of the CO in the photoproduct, so that the only effect on the CO position is a small shift away from the bound position. Teng *et al.* performed the x-ray data collection in the dark immediately after the light flash. This gives also a higher fraction of rebonded CO molecules in comparison to permanent illumination experiments.

Extended x-ray absorption fine structure experiments have yielded CO displacements between 0.05 and 0.07 A in the photoproduct (6, 8–10). They are thus in disagreement with the distant position of the CO in the photoproduct and in support of a closer position. A critical discussion of the problems of the extended x-ray absorption fine structure method to obtain the photoproduct structure has been given earlier by Fiamingo and Alben (33).

Our work shows that the discrepancies in the position of the photodissociated CO between the two earlier structure determinations of Mb*CO are not due to crystal packing effects because our position 2 of the CO in monoclinic crystals is identical to the location of the CO in P6 crystals. We also find a substantial out-of-plane displacement of the heme iron. However, from our data set we were not able to detect any changes in the position of the distal histidine imidazole side chain. Schlichting *et al.* (11) reported a shift of 1.7 A for their P6 structure, which we should have easily detected. A possible explanation involves either the slightly altered structure because of the mutation or different crystal packing forces.

Recently it has been shown that extended illumination of MbCO at low temperature leads to a light-induced relaxation (7, 34, 35) that is similar to the thermally induced relaxation above 200 K (34, 35). Because the structure of Mb*CO is very close to MbCO we do not believe that such effects influence our results.

This work was supported by the Bundesministerium für Forschung und Technologie (BMFT), Projektträger Synchrotronstrahlung, DESY (Hamburg), and the Fonds der Chemie. G.U.N. acknowledges support from National Institutes of Health Grant GM 18051. R.T.S. thanks the European Molecular Biology Laboratory for a fellowship.

1. Austin, R. H., Beeson, K. W., Eisenstein, L., Frauenfelder, H. & Gunsalus I. C. (1975) *Biochemistry* **14,** 5355–5373.
2. Ansari, A., Berendzen, J., Bowne, S. F., Frauenfelder, H., Iben, I. E. T., Sauke, T. B., Shyamsunder, E. & Young, R. D. (1985) *Proc. Natl. Acad. Sci. USA* **82,** 5000–5004.
3. Nienhaus, G. U., Mourant, J. R. & Frauenfelder, H. (1992) *Proc. Natl. Acad. Sci. USA* **89,** 2902–2906.
4. Ormos, P., Braunstein, D., Frauenfelder, H., Hong, M. K., Lin, S. L., Sauke, T. B. & Young, R. D. (1988) *Proc. Natl. Acad. Sci. USA* **85,** 8492–8496.
5. Winkler, H., Franke, M., Trautwein, A. X. & Parak, F. (1990) *Hyperfine Interact.* **58,** 2405–2411.
6. Chance, B., Fischetti, R. & Powers L. (1983) *Biochemistry* **22,** 3820–3829.
7. Powers, L., Sessler, J. L., Woolery, G. L. & Chance, B. (1984) *Biochemistry* **23,** 5519–5523.
8. Powers, L., Chance, B., Chance, M., Campbell, B., Friedman, J., Khalid, S., Kumar, C., Naqui, A., Reddy, K. S. & Zhou, Y. (1987) *Biochemistry* **26,** 4785–4796.
9. Teng, T. Y., Huang, H. W. & Olah, G. A. (1987) *Biochemistry* **26,** 8066–8072.
10. Della Longa, S., Ascone, I., Fontaine, A., Congiu Castellano, A. & Bianconi, A. (1994) *Eur. Biophys. J.* **23,** 361–368.
11. Schlichting, I., Berendzen, J., Phillips, G. N., Jr., & Sweet, R. M. (1994) *Nature (London)* **317,** 808–812.
12. Teng, T. Y., Srajer, V. & Moffat, K. (1994) *Nat. Struct. Biol.* **1,** 701–705.
13. Kendrew, J. C. & Parrish, R. G. (1956) *Proc. R. Soc. London A* **238,** 305–324.
14. Parak, F., Thomanek, U. F., Bade, D. & Wintergerst, B. (1977) *Z. Naturforsch. C* **32,** 507–512.
15. Parak, F., Hartmann, H., Aumann, K. D., Reuscher, H., Rennekamp, G., Bartunik, H. & Steigemann, W. (1987) *Eur. Biophys. J.* **15,** 237–249.
16. Bücher, T. & Kaspers, J. (1947) *Biochim. Biophys. Acta* **1,** 21–34.
17. Otwinowski, Z. (1993) in *Data Collection and Processing*, eds. Sawjer, L., Isaacs, N. & Bailey, S. S. (SERC Daresbury Lab., Warrington, U.K.), pp. 56–62.
18. Nienhaus, G. U., Drepper, F., Parak, F., Mössbauer, R. L., Bade, D. & Hoppe, W. (1987) *Nucl. Instrum. Methods A* **256,** 581–586.
19. Schwager, P. & Bartels, K. (1977) *The Rotation Method in Crystallography* (North–Holland, Amsterdam).
20. Konnert, J. H. & Hendrickson, W. A. (1980) *Acta Crystallogr. A* **6,** 344–355.
21. Hartmann, H., Steigemann, W., Reuscher, H. & Parak, F. (1987) *Eur. Biophys. J.* **14,** 337–348.
22. Parak, F., Hartmann, H., Schmidt, M., Corongiu, G. & Clementi, E. (1992) *Eur. Biophys. J.* **21,** 313–320.
23. Kuriyan, J., Wilz, S., Karplus, M. & Petsko, G. A. (1986) *J. Mol. Biol.* **192,** 133–154.
24. Luzzati, V. (1952) *Acta Crystallogr.* **5,** 802–810.
25. Alben, J. O., Beece, D., Bowne, S. F., Eisenstein, L., Frauenfelder, H., Good, D., Marden, M. C., Moh, P. P., Reinisch, L., Reynolds, A. H. & Yue, K. T. (1980) *Phys. Rev. Lett.* **44,** 1157–1160.
26. Steigemann, W. & Weber, E. (1979) *J. Mol. Biol.* **127,** 309–338.
27. Peng, S. M. & Ibers, J. A. (1976) *J. Am. Chem. Soc.* **98,** 8032–8036.
28. Cheng, X. & Schoenborn, B. P. (1990) *Acta Crystallogr. A* **46,** 195–208.
29. Mourant, J. R., Braunstein, D. P., Chu, K., Frauenfelder, H., Nienhaus, G. U., Ormos, P. & Young, R. D. (1993) *Biophys. J.* **65,** 1496–1507.
30. Oldfield, E., Guo, K., Augspurger, J. D. & Dykstra, C. E. (1991) *J. Am. Chem. Soc.* **113,** 7537–7541.
31. Ansari, A., Berendzen, J., Braunstein, D., Cowen, B. R., Frauenfelder, H., Hong, M. K., Iben, I. E. T., Johnson, J. B., Ormos, P., Sauke, T. B., Scholl, R., Schulte, A., Steinbach, P. J., Vittitow, J. & Young, R. D. (1987) *Biophys. Chem.* **26,** 337–355.
32. Young, R. D., Frauenfelder, H., Johnson, J. B., Lamb, D. C., Nienhaus, G. U., Philipp, R. & Scholl, R. (1991) *Chem. Phys.* **158,** 315–327.
33. Fiamingo, F. G. & Alben, J. O. (1985) *Biochemistry* **24,** 7964–7970.
34. Nienhaus, G. U., Mourant, J. R., Chu, K. & Frauenfelder, H. (1994) *Biochemistry* **33,** 13413–13430.
35. Chu, K., Ernst, R. M., Frauenfelder, H., Mourant, J. R., Nienhaus, G. U. & Philipp, R. (1995) *Phys. Rev. Lett.* **74,** 2607–2610.